ORIGINAL ARTICLE

Open Access

Properties of multi-GNSS uncalibrated phase delays with considering satellite systems, receiver types, and network scales

Ping Zeng[1], Zhetao Zhang[1*], Yuanlan Wen[1], Xiufeng He[1], Lina He[1], Muzi Li[2] and Wu Chen[3]

Abstract

The Wide-Lane (WL) and Narrow-Lane (NL) Uncalibrated Phase Delays (UPDs) are the prerequisites in the traditional Precise Point Positioning (PPP) Ambiguity Resolution (AR). As the generation mechanism of various biases becomes more complex, we systematically studied the impact factors of four satellite systems WL and NL UPDs from the perspective of parameter estimation. Approximately 100 stations in a global network are used to generate the UPDs. The results of different satellite systems show that the estimation method, update frequency, and solution mode need to be treated differently. Two regional networks with different receiver types, JAVAD, and Trimble, are also adopted. The results indicate that the receiver-dependent bias has an influence on UPD estimation. Also, the hardware delays can inhibit the satellite-side UPDs if these receiver-specific errors are not fully deployed or even misused. Furthermore, the temporal stability and residual distribution of NL UPDs are significantly enhanced by utilizing a regional network, with the improvements by over 68% and 40%, respectively. It demonstrates that different network scales exhibit the different implication of unmodeled errors, and the unmodeled errors cannot be ignored and must be handled in UPD estimation.

Keywords WL UPD, NL UPD, Satellite system, Receiver type, Network scale

Introduction

As of 2023, more than 120 global navigation satellites from Global Positioning System (GPS), BeiDou Navigation Satellite System (BDS), Galileo navigation satellite system (Galileo), and GLObal NAvigation Satellite System (GLONASS) can be used for high-precision positioning (Yang et al., 2020). As a prominent technique for high-precision positioning with a single Global Navigation Satellite System (GNSS) receiver, Precise Point Positioning (PPP) (Zumberge et al., 1997) has been widely used in various fields, such as earthquake (Jin et al., 2019), tsunami (Inazu et al., 2016), precise positioning (Shinghal & Bisnath, 2021), crustal deformation (Zheng et al., 2021), and structural health monitoring (Ju et al., 2022), etc. However, due to the Uncalibrated Phase Delay (UPD) in phase observation, the undifferenced ambiguity parameter has lost the integer property (Blewitt, 1998). Hence, the convergence time of over 30 min is usually required for PPP to achieve centimeter-level accuracy (Kouba & Héroux, 2001). To shorten the convergence time and improve the positioning accuracy, the PPP Ambiguity Resolution (PPP-AR) technique was developed in last decade.

There are several methods to implement PPP-AR, and it has been demonstrated that there are connections between the various methods. In general, these methods can be divided into two categories. One is

*Correspondence:
Zhetao Zhang
ztzhang@hhu.edu.cn
[1] School of Earth Sciences and Engineering, Hohai University, Nanjing 211100, China
[2] Shanghai Aerospace Control Technology Institute, Shanghai 201109, China
[3] Department of Land Surveying and Geo-Informatics, The Hong Kong Polytechnic University, Hong Kong, China

Zeng *et al. Satellite Navigation*   (2023) 4:19

Page 2 of 15

based on the undifferenced and uncombined observations (Teunissen et al., 2010; Zhang et al., 2011; Khodabandeh & Teunissen, 2015), and the other is based on the Ionosphere-Free (IF) combination, which includes the integer-recovery clock method (Laurichesse et al., 2009), the decoupled-clock method (Collins et al., 2008), and the UPD method (Ge et al., 2008). Considering that the server-side is not concerned with the time behaviors of ionospheric parameters, the IF combination methods are widely used. In the integer-recovery clock method, the Wide-Lane (WL) ambiguities are fixed by applying the WL UPD products, then the Narrow-Lane (NL) ambiguities are resolved before the clock estimation. However, the process of network solution with ambiguity-fixed in integer clock estimation is a little complicated (Blewitt, 2008). Similarly, Collins et al. (2008) developed a decoupled clock model, which is characterized by code clocks differing from carrier-phase clocks. Correspondingly, PPP users can obtain an ambiguity-fixed solution with decoupled-clock products of code clocks, phase clocks, and WL biases. From the perspective of product estimation strategy, the decoupled-clock method is more rigorous than the integer-recovery clock method because it considers the day-boundary clock jumps caused by code biases (Liu et al., 2022). Therefore, the systematic errors in the pseudorange observations can be significantly reduced by applying the code clock. Unfortunately, there are no decoupled clock products available for PPP users at present. In addition, like the integer-recovery clock method, the decoupled-clock method is inefficient due to the heavy computational burden when processing the massive networks. By contrast, Ge et al. (2008) proposed a single-difference between-satellites method that eliminates the receiver biases through a single-differencing. The integer property is recovered by sequentially correcting the satellite WL and NL UPDs. Compared with the integer-recovery clock and decoupled-clock method, the UPD method is compatible with the International GNSS Service (IGS) products, and the user side does not need to be redesigned, which is more convenient. Correspondingly, based on the traditional UPD model, Geng et al. (2019b) proposed a modified phase clock/bias model to enable undifferenced ambiguity resolution. This model can be regarded as a variant of the integer clock model but solves the incompatibility problem with IGS products. Users can use the phase clock and phase bias products in conjunction with the precise orbit products provided by Wuhan University to implement high accuracy PPP-AR with the open-source software of PRIDE-PPPAR (Geng et al., 2019a). However, as more and more Analysis Centers (ACs) provide multi-constellation orbit and clock products, it is still a challenge for users to fix the ambiguities by using precise products of other ACs. Hence, the UPD estimation is still one of the major procedures in PPP-AR.

Since the accuracy of precise orbit, clock products, and UPDs is crucial for PPP-AR, many researchers have made great efforts to obtain more accurate UPDs based on IGS products. Geng et al. (2012) proposed an improved method to generate the NL UPDs with the ambiguities derived from a double-differenced ambiguity-fixed GPS network solution and found it more effective when fewer stations are involved in the UPD estimation. With the full operation of BeiDou-2 Navigation Satellite System (BDS-2), Liu et al. (2017) estimated the BDS UPDs using a regional network, and the ambiguity fixing rate was improved when the BDS Inclined Geosynchronous Satellite Orbit (IGSO) and Medium Earth Orbit (MEO) satellites were added in ambiguity resolution. Although there are many studies on the method of UPD estimation and many ACs providing UPD products with the main aims of shortening the convergence time and improving the PPP accuracy, limited studies focused on the properties of UPDs. Furthermore, the UPD estimation may absorb some unexpected biases when the observation types get involved that are different among a particular pair of observed satellites (Schaer et al., 2021). Therefore, the UPD method is not theoretically rigorous and can cause fluctuations in the estimation results. It is necessary to analyze these issues because of some differences among the four satellite systems, such as the different signal types, different accuracy of orbit and clock products, etc. In addition, there are currently over 500 Multi-GNSS EXperiment (MGEX) stations around the world equipped with various receiver types. The studies have shown that the receiver-dependent UPD deviation can cause significant positioning errors (Cui et al., 2021). The fluctuations of NL UPDs are also caused by the residual systematic errors such as tropospheric delays, multipath, and other errors. These unmodeled errors are spatially dependent (Li et al., 2018). Therefore, different receiver types and network scales will have different unmodeled errors which lead to the different quality of UPDs.

We systematically study the impact factors of GPS/BDS/Galileo/GLONASS WL and NL UPDs from the perspective of parameter estimation. This paper for the first time comprehensively analyzes the properties of GPS/BDS/Galileo/GLONASS WL and NL UPDs. Specifically, the impacts of satellite systems, receiver types, and network scales are all considered. By using the different satellite systems, different receiver types, and different network scales, we generate the corresponding WL and NL UPDs to interpret some properties more comprehensively.

Methodology

In this section, the basic multi-GNSS observation equations are presented, and then the detail of WL and NL ambiguity resolution are given. Finally, the methodology to estimate WL and NL UPDs is discussed, where the impacts of different satellite systems, receiver types, and network scales are all considered.

Multi-GNSS observation equations

For GPS/BDS/Galileo/GLONASS data, the code and phase observations for a receiver r and satellite s on frequency i at a certain epoch can be expressed as follows (Leick et al., 2015; Teunissen & Montenbruck, 2017)

$$P_{r,i}^s = \rho_r^s + ct_r - ct^s + \xi_{r,i} - \xi^{s,i} + \mu_i I_{r,1}^s + T_r^s + \epsilon_{r,i}^s \tag{1}$$

$$\phi_{r,i}^s = \rho_r^s + ct_r - ct^s + \lambda_i \left(\zeta_{r,i} - \zeta^{s,i} \right) + \lambda_i N_{r,i}^s - \mu_i I_{r,1}^s + T_r^s + \in_{r,i}^s \tag{2}$$

where P and ϕ are the code and phase observations, respectively; ρ is the geometric distance between satellite to receiver; c is the speed of light in a vacuum; t_r and t^s are the receiver and satellite clock offsets, respectively; ξ and ζ are the code and phase hardware delays, respectively; λ and N are the wavelength and ambiguity, respectively; I and T are the ionospheric and tropospheric delays, respectively, with $\mu_i = \lambda_i^2/\lambda_1^2$; ϵ and $\in$ are the code and phase observation noise as well as unmodeled errors, respectively. The Phase Center Offset (PCO) and Phase Center Variation (PCV) (Schmid et al., 2005), phase windup (Wu et al., 1993), tidal loading, relativistic effect, and earth rotation can be corrected by the existing empirical models.

In PPP applications, the IF combination is widely used since it can eliminate the first-order ionospheric delays. The code and phase IF combination between frequencies i and j can be defined as

$$P_{r,\mathrm{IF}}^s = \frac{f_i^2}{f_i^2 - f_j^2} P_{r,i}^s - \frac{f_j^2}{f_i^2 - f_j^2} P_{r,j}^s \tag{3}$$

$$\phi_{r,\mathrm{IF}}^s = \frac{f_i^2}{f_i^2 - f_j^2} \phi_{r,i}^s - \frac{f_j^2}{f_i^2 - f_j^2} \phi_{r,j}^s \tag{4}$$

where i and j $(i \neq j)$ are the frequencies. Hence, the IF PPP is the most popular model on the user side. Also, the UPD estimators are usually based on the IF model including in this study. According to (1) and (2), the IF code and phase observation equations are given as

$$P_{r,\mathrm{IF}}^s = \rho_r^s + ct_r - ct^s + \xi_{r,\mathrm{IF}} - \xi^{s,\mathrm{IF}} + T_r^s + \epsilon_{r,\mathrm{IF}}^s \tag{5}$$

$$\phi_{r,\mathrm{IF}}^s = \rho_r^s + ct_r - ct^s + \lambda_{\mathrm{IF}} \left(\zeta_{r,\mathrm{IF}} - \zeta^{s,\mathrm{IF}} \right) + \lambda_{\mathrm{IF}} N_{r,\mathrm{IF}}^s + T_r^s + \in_{r,\mathrm{IF}}^s \tag{6}$$

It is worth noting that in the case of multi-constellation GNSS, there exist the differences of IF code hardware delays between different constellations for a receiver. These differences refer to the Inter-System Biases (ISB). As usual, the ISB parameters can be assimilated into the individual receiver clock parameters in each constellation (Zhang et al., 2021). Besides, the IF phase hardware delays are also different, and these differences are absorbed by the IF ambiguities (Li et al., 2021). For the GLONASS satellites with different frequency factors, the receiver code and phase hardware delays are also different, which are called as Inter-Frequency Biases (IFB). The receiver IFB is also assimilated into the receiver clock parameter, and the IFB parameters need to be set for each satellite.

Multi-GNSS WL and NL ambiguity resolution

When estimating the multi-GNSS UPDs, the first step is to calculate the float WL ambiguities. Specifically, the Melbourne-Wübeena (MW) combination is used, which consists of one phase WL combination and one code NL combination (Melbourne, 1985; Wübbena, 1985) as

$$L_{r,\mathrm{MW}}^s = \phi_{r,w}^s - P_{r,n}^s \tag{7}$$

with $\phi_{r,w}^s = \frac{f_i}{f_i - f_j} \phi_{r,i}^s - \frac{f_j}{f_i - f_j} \phi_{r,j}^s$, and $P_{r,n}^s = \frac{f_i}{f_i + f_j} P_{r,i}^s + \frac{f_j}{f_i + f_j} P_{r,j}^s$, where $L_{r,\mathrm{MW}}^s$ is the MW combination for the receiver r and satellite s. The MW combination is a geometry-free and ionospheric-free combination. Hence, the most advantage of MW combination is that it eliminates the geometric term and first-order ionospheric term with larger wavelength compared with the raw phase observations. Accordingly, the float WL ambiguities can be estimated as

$$\check{N}_{r,w}^s = \frac{\phi_{r,w}^s - P_{r,n}^s}{\lambda_w} \tag{8}$$

with $\lambda_w = \frac{c}{f_i - f_j}$, and $N_{r,w}^s = N_{r,i}^s - N_{r,j}^s$, where $\check{N}$ is the float ambiguity.

The second step is to fix the WL ambiguities in (8). Thanks to the relatively long wavelength (e.g., 86 cm for GPS L1 and L2 signals), the float WL ambiguities containing the hardware delays can be fixed by rounding within a certain period. The fixed WL ambiguities can be estimated as follows (Ge et al., 2008)

$$\hat{N}_{r,w}^s = \left\langle \frac{\sum_k^{k+m-1} \check{N}_{r,w}^s(k)}{m} \right\rangle \tag{9}$$

Zeng *et al. Satellite Navigation*   (2023) 4:19

Page 4 of 15

where $\hat{N}$ is the fixed ambiguity; $\langle\cdot\rangle$ is the operator of rounding; k and m are the starting epoch and the epoch number, respectively. The STandard Deviation (STD) of fixed WL ambiguities reads

$$\sigma_{\hat{N}^s_{r,w}} = \sqrt{\frac{\sum_k^{k+m-1}\left[\check{N}^s_{r,w}(k) - \hat{N}^s_{r,w}\right]^2}{m}} \tag{10}$$

The third step is, to obtain the float NL ambiguities, which needs to estimate the IF ambiguities based on (5) and (6). According to the IGS analysis tradition, the code IF hardware delays on the satellite-end are assimilated into the satellite clock offset. Hence, after the correction for satellite clock offsets by using the corresponding precise satellite clock products, the equivalent float IF ambiguities can be expressed as

$$\check{N}^s_{r,\mathrm{IF}} = N^s_{r,\mathrm{IF}} + b_{r,\mathrm{IF}} - b^{s,\mathrm{IF}} \tag{11}$$

with $b_{r,\mathrm{IF}} = \zeta_{r,\mathrm{IF}} - \xi_{r,\mathrm{IF}}/\lambda_{\mathrm{IF}}, b^{s,\mathrm{IF}} = \zeta^{s,\mathrm{IF}} - \xi^{s,\mathrm{IF}}/\lambda_{\mathrm{IF}}$.

The float NL ambiguities can then be deduced according to the fixed WL ambiguities and equivalent float IF ambiguities are as follows

$$\check{N}^s_{r,n} = \frac{f_1+f_2}{f_1}\check{N}^s_{r,\mathrm{IF}} - \frac{f_2}{f_1-f_2}\hat{N}^s_{r,w} \tag{12}$$

The STD of float NL ambiguities is

$$\sigma_{\check{N}^s_{r,n}} = \frac{f_1+f_2}{f_1}\sigma_{\check{N}^s_{r,\mathrm{IF}}} \tag{13}$$

The float NL ambiguities can also be fixed in the similar way as shown in (9).

Estimation of WL and NL UPDs

After the WL and NL ambiguities are resolved, the WL and NL UPDs can be obtained. Since the WL and NL UPDs are estimated almost in the same way, for the sake of simplicity, the symbol denoting the WL or NL is not given. Without loss of generality, the float ambiguity can be expressed as

$$\check{N}^s_r = \hat{N}^s_r + b_r + b^s + u^s_r \tag{14}$$

where b_r and b^s are the receiver and satellite UPD like in (11), respectively; u^s_r is the combined error term containing the observation noise and unmodeled errors.

Assuming there are r reference stations and s observable satellites in a network, the observation equation can be written as

$$\begin{bmatrix} \check{\boldsymbol{N}}_1 \\ \vdots \\ \check{\boldsymbol{N}}_r \end{bmatrix} = \begin{bmatrix} \hat{\boldsymbol{N}}_1 \\ \vdots \\ \hat{\boldsymbol{N}}_r \end{bmatrix} + \begin{bmatrix} \boldsymbol{I}_r \otimes \boldsymbol{e}_s & \boldsymbol{e}_r \otimes \boldsymbol{I}_s \end{bmatrix} \begin{bmatrix} \boldsymbol{b}_r \\ \boldsymbol{b}^s \end{bmatrix} + \begin{bmatrix} \boldsymbol{u}_1 \\ \vdots \\ \boldsymbol{u}_r \end{bmatrix} \tag{15}$$

with $\check{\boldsymbol{N}}_r = \left[\check{N}^1_r, \check{N}^2_r, \cdots, \check{N}^s_r\right]^{\mathrm{T}}, \hat{\boldsymbol{N}}_r = \left[\hat{N}^1_r, \hat{N}^2_r, \cdots, \hat{N}^s_r\right]^{\mathrm{T}},$ $\boldsymbol{b}_r = [b_1, b_2, \cdots, b_r]^{\mathrm{T}}, \quad \boldsymbol{b}^s = [b^1, b^2, \cdots, b^s]^{\mathrm{T}}, \quad$ and $\boldsymbol{u}_r = \left[u^1_r, u^2_r, \cdots, u^s_r\right]^{\mathrm{T}},$ where $\boldsymbol{I}_r$ is the r-order identity matrix, and $\boldsymbol{e}_s$ is the $(s+1)$-column vector with all one elements; $\otimes$ is the operator of Kronecker product. Unfortunately, the observation Eq. (15) has a rank defect of 1 because of the linear dependence between receiver and satellite UPD. In order to avoid the problem of rank deficiency, one extra constraint is introduced, e.g., setting the UPD of reference satellite to 0 (Zhang & Li, 2013). Finally, the satellite and receiver UPDs can be estimated by the Least Squares (LS) criterion. It is worth noting that, according to (15), the correlations among UPDs can be expressed with a variance-covariance matrix.

From (14) and (15), the WL and NL UPDs are influenced by the receiver, satellite, and error terms to some extent. It is evident that the behaviors of UPDs are dependent on the satellite types. Hence, the amplitude and stability of the UPDs for GPS, BDS, Galileo, and GLONASS differ from each other. The receiver also has impacts on the UPDs. The reason is that the solution mode in (15) often relies on the property of the hardware delays, including the receiver-specific hardware delay. In addition, the receiver-dependent bias also influences the UPD estimation. The unmodeled errors especially the residual atmospheric delays and multipath effects are often ignored in estimating the UPDs. They will affect the accuracy of UPDs if the errors are significant in a specific network.

Data and experiment

The observations of GPS/BDS/Galileo/GLONASS from the MGEX and Europe Reference Frame (EUREF) are used to estimate global and regional UPDs with the same precise products offered by GFZ (Deutsches GeoForschungsZentrum Potsdam). As shown in Fig. 1, there are approximately 100 MGEX stations equipped with several receiver types. In order to analysis the impacts of different receivers on UPD estimation, the stations selected from EUREF are divided into two networks. As can be seen in Fig. 2 and 26 stations (red circles) are equipped with JAVAD receivers, while 30 stations (blue triangles) are equipped with Trimble receivers. All these stations can track the dual-frequency observations of GPS/BDS/Galileo/GLONASS with a 30s sampling interval. Thirty days of observations from June 1st to 30th in 2021 were
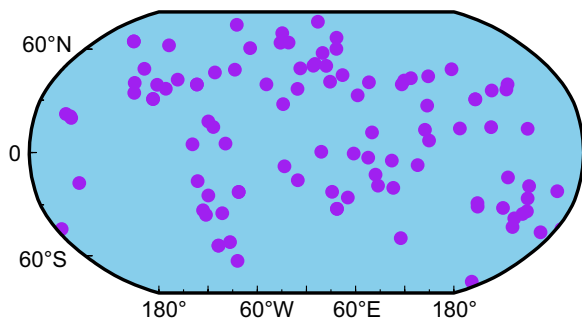
Zeng *et al. Satellite Navigation*   (2023) 4:19

Page 5 of 15

Fig. 1 Distribution of MGEX stations which are used for global UPD estimation
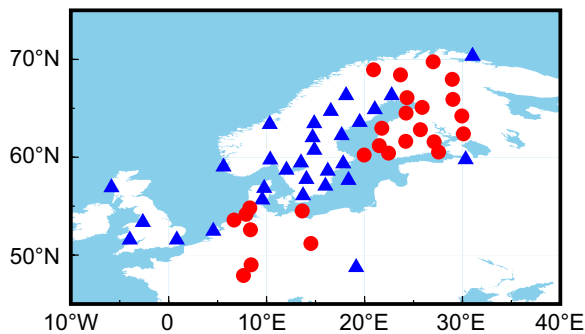

Fig. 2 Distribution of the EUREF stations which are used for regional UPD estimation. The red circles and blue triangles denote the stations equipped with JAVAD and Trimble receivers, respectively

collected. Generally, the static PPP is used to estimate IF ambiguities and WL ambiguities for each station. To obtain better IF ambiguities, the coordinates of MGEX stations are fixed to igs21P2160.snx with

tightly constrained, while the EUREF stations are fixed to the GPS-only daily solution with 2 cm constrains. For the BDS-2, the code observations were corrected by following Wanninger and Beer (2015). The other details of the processing strategies for UPD estimation are shown in Table 1.

Results and discussion

In this section, we generate the GPS/BDS/Galileo/GLO-NASS WL and NL UPDs by using different satellite systems, receiver types, and network scales. Subsequently, the properties of WL and NL UPDs are comprehensively interpreted.

Analysis of UPD estimators considering the impacts of satellite systems

The properties of WL and NL UPDs generated by different satellite systems in the global network are illustrated. Figure 3 shows the series of the GPS, BDS, Galileo, and GLONASS daily WL UPDs from Day of Year (DOY) 152 to 181, 2021. To keep the consistency of the time series, the WL UPDs of some satellites are adjusted by adding ± 1 cycle. As can be seen from the left-upper of Fig. 3, the mean standard deviations of GPS WL UPDs are approximately 0.018 cycles, where the largest STDs is 0.046 cycles for G28. The right-bottom of Fig. 3 indicates that the GLONASS WL UPDs vary significantly within the period of 30 days. The mean STDs of GLO-NASS UPDs reach 0.070 cycles, and the largest STDs up to 0.130 cycles for R21. The Galileo and BDS WL UPDs are illustrated at the bottom-left and upper-right of Fig. 3. The mean STDs of Galileo is approximately 0.024 cycles, while the BDS is 0.019 cycles. The GPS WL UPDs

Table 1 Processing strategies for UPD estimation

| Items	Strategies
Observation	IF combination
Frequency	GPS: L1/L2; BDS: B1I/B3I; Galileo: E1/E5a; GLONASS: G1/G2
Sampling rate	30 s
Cutoff elevation	7°
Satellite orbit and clock	GFZ final products
Tropospheric delay	Saastamoinen model with Global Mapping Function (GMF), and the Zenith Wet Delay (ZWD) estimated as random walk noise.
Tidal displacement	International Earth Rotation Service (IERS) conventions 2010
Antenna PCO and PCV	igs14_2148.atx
Phase wind-up	Corrected
Differential Code Bias (DCB)	CODE (Center for Orbit Determination in Europe) products
UPD estimation	WL: daily constant NL: 15 min-session constant
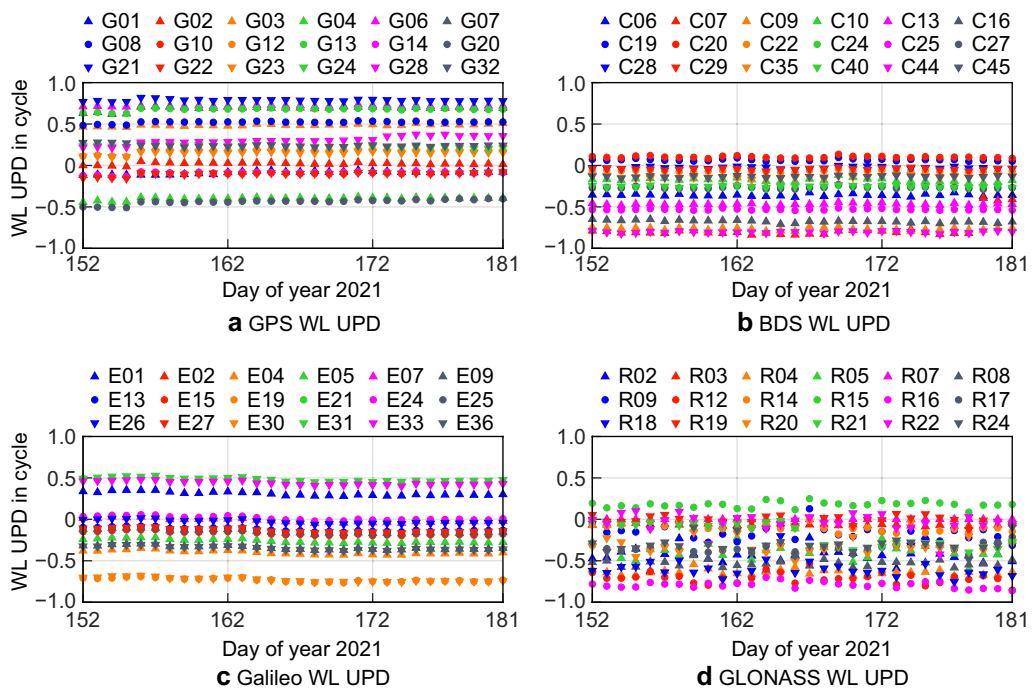
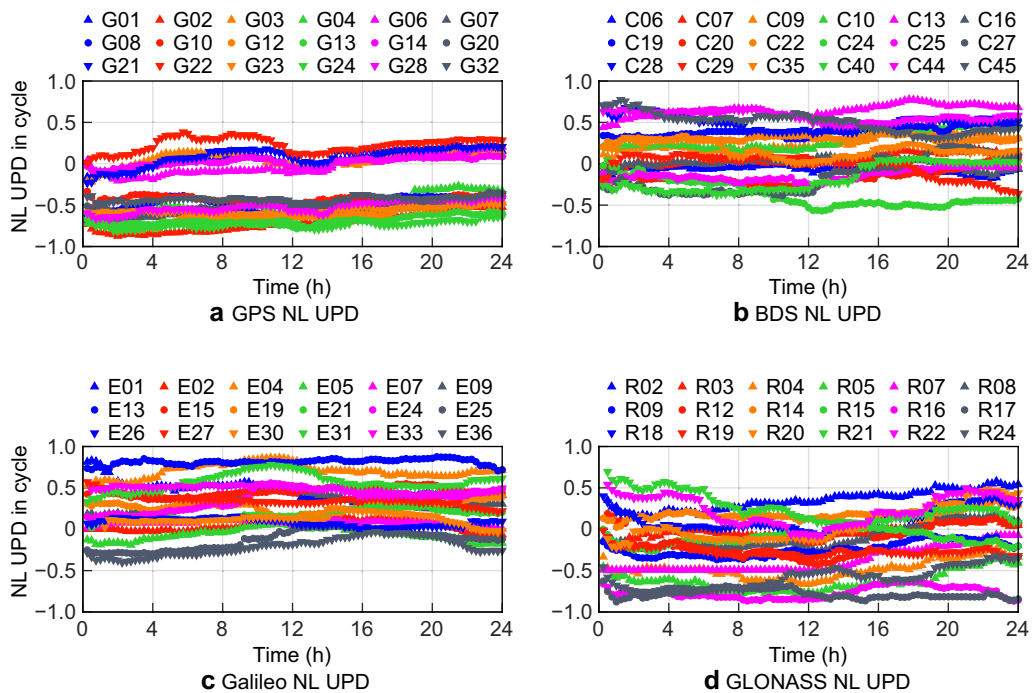**Fig. 3** GPS (**a**), BDS (**b**), Galileo (**c**), and GLONASS (**d**) WL UPDs estimated in the global network from DOY 152 to 181 of 2021

Fig. 4 GPS (**a**), BDS (**b**), Galileo (**c**), and GLONASS (**d**) NL UPDs estimated by global network on DOY 152 of 2021

Zeng *et al. Satellite Navigation*   (2023) 4:19

Page 7 of 15

Table 2 Usage rate of WL and NL float ambiguities in the global network on DOY 152 of 2021

System	WL usage rates in the global network (%)			NL usage rates in the global network (%)		
	Average	Maximum	Minimum	Average	Maximum	Minimum
GPS	97.7	100	87.3	98.1	99.5	96.3
BDS	92.9	100	75.4	91.6	98.8	77.0
Galileo	97.6	100	91.6	97.3	99.7	89.8
GLONASS	72.0	90.5	60.0	88.2	94.9	76.7

have the best performance in terms of temporal stability. In addition, Galileo and BDS have more stable WL UPDs than GLONASS. This is because the code and carrier phase IFBs are included in the GLONASS WL UPDs.

Figure 4 illustrates the NL UPD series of four satellite systems on DOY 152 of 2021. The mean STDs of GPS and Galileo NL UPDs are approximately 0.075 and 0.080 cycles, respectively, while the ones of BDS and GLONASS are 0.096 and 0.099 cycles. GPS and Galileo show the similar performance in terms of temporal stability and have better NL UPDs than GLONASS and BDS. The difference is probably attributed to the precise product, signal type, and signal quality in different satellite systems.

To further analyze the properties of UPDs of four satellite systems, the usage rate of ambiguities is adopted which is defined as the ratio of the valid ambiguities over all ambiguities. The usage rates of WL and NL ambiguities in the global network are given in Table 2. We can find that the average usage rates of WL ambiguities for GPS, BDS, Galileo, and GLONASS are 97.7%, 92.9%, 97.6%, and 72.0%, respectively, while those for NL ambiguities are 98.1%, 91.6%, 97.3%, and 88.2%. The average usage rates of both WL and NL UPDs for GPS are higher than other satellite systems. For GLONASS, the R07 has the highest usage rates of WL and NL ambiguities, i.e., 90.5% and 94.9%, respectively. However, except for R07, the others perform poorly in WL and NL ambiguities usage rates. For Galileo, all satellites have high usage rates. Even the minimum usage rates of WL and NL ambiguities are up to 91.6% and 89.8%, respectively. The main reason is due to the high-quality observations for Galileo satellites. For BDS, the usage rates of BeiDou-3 Navigation Satellite System (BDS-3) MEO satellites are higher than those of BDS-2 IGSO satellites. It is reasonable because the precise orbit and clock accuracy of BDS-3 MEO satellites are generally higher than that of BDS-2 IGSO satellites.

The residuals of WL and NL ambiguities can be used to evaluate the quality of UPDs. After the UPDs are removed from WL and NL ambiguities, the ambiguities should be close to integers. Then, the residuals can be expressed by the fractional parts of the float
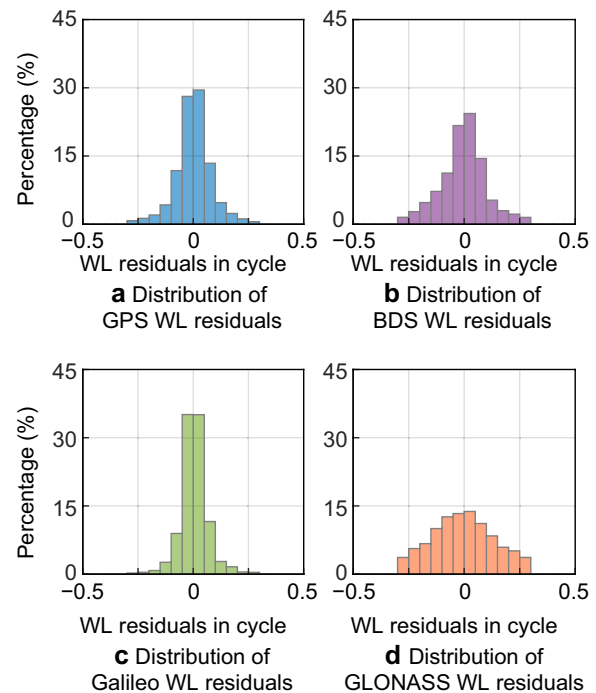
Fig. 5 Histograms of the GPS (**a**), BDS (**b**), Galileo (**c**), and GLONASS (**d**) WL residuals in the global network on DOY 152 of 2021

ambiguities. As shown in Fig. 5, the GPS and Galileo have roughly the same distribution of WL residuals. By contrast, the GLONASS and BDS have more discrete distribution. We can find in Table 3, Galileo has the best performance in the distribution of the residuals, and 96.1% of the residuals are within ± 0.15 cycles and 99.4% within ± 0.25 cycles. In contrast, the corresponding results for GLONASS are 69.6% and 92.7%. It demonstrates that the IFBs can inhibit the UPD estimation.

Figure 6 shows the distribution of NL ambiguities residuals. Compared with the WL residuals, the NL residuals have no significant differences among four satellite systems. We can find in Table 3 that all the percentages of NL residuals within ± 0.15 and ± 0.25 cycles are higher than 80% and 99%, respectively. In addition, four satellite
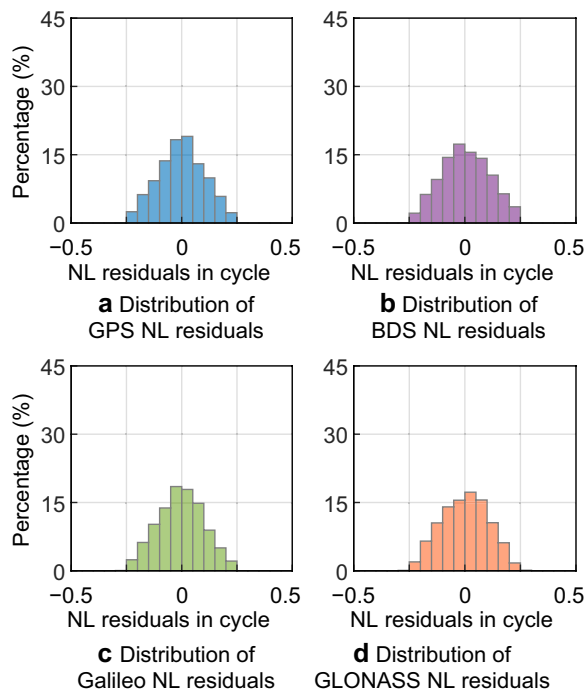
Zeng *et al. Satellite Navigation*   (2023) 4:19

Page 8 of 15

Fig. 6 Histograms of the GPS (**a**), BDS (**b**), Galileo (**c**), and GLONASS (**d**) NL residuals in the global network on DOY 152 of 2021

series of the daily WL UPDs generated in the network with 26 JAVAD receivers from DOY 152 to 181 of 2021. The mean STDs for GPS, BDS, Galileo, and GLONASS are approximately 0.026, 0.032, 0.016, and 0.035 cycles, respectively. For another regional network with 30 Trimble receivers, the estimated WL UPDs are shown in Fig. 8. The corresponding mean STDs are 0.024, 0.020, 0.034, and 0.026 cycles. These results indicate that the WL UPDs estimated in two networks have a high stability, but there are some differences between them. We can find that the GPS, GLONASS, and BDS WL UPDs estimated in the network equipped with Trimble receivers are slightly more stable than those with JAVAD receivers. The reason is probably that the receiver-dependent biases, such as residuals of antenna PCO and receiver noise, contaminate the satellite UPDs.

By comparing the Figs. 3 and 7, we can find that the GLONASS WL UPDs estimated with JAVAD receivers are more stable than that those estimated in the global network with several receiver types. Thanks to the homogeneous JAVAD receivers, the STDs decrease from 0.070 cycles to 0.035 cycles. By comparing the Figs. 3 and 8, the GLONASS WL UPDs estimated with Trimble receivers have similar results, and the stability of WL UPDs is improved by approximately 62.7%. Thus, homogeneous receivers can significantly reduce the impact of IFB on the UPD estimation. The significant improvement is due to the unmodeled error of GLONASS IFB for homogeneous receivers is similar, which can be absorbed into the datum of UPD. It indicates that appropriate solution strategies are also crucial for UPD estimation.

The usage rates of WL float ambiguities in the two regional networks are given in Table 4. The average usage rates of WL float ambiguities in the regional network with JAVAD receivers are higher than those in the regional network with Trimble receivers. In the former network, the usage rates of WL float ambiguities for all GPS and Galileo satellites are 100%, while in the latter network the usage rates range from 96.7% (G03) to 100% (G06) for GPS, and 93.3% (E13) to 100% (E02) for Galileo.

Figure 9 illustrates the distribution of WL ambiguities residuals in the network with JAVAD receivers. Four satellite

systems have roughly the same STDs of NL ambiguities residuals. Since the WL ambiguities are already fixed, the quality of NL UPDs is dominated by the precision of the IF ambiguities. In general, higher IF ambiguities usage rates can improve the accuracy of NL UPDs, but the prerequisite is that the IF ambiguities have minor unmodeled errors. In conclusion, the estimation method, update frequency, and solution mode of UPD need to be treated differently for different satellite systems.

Analysis of UPD estimators considering the impacts of receiver types

The UPDs are also estimated in two regional networks, i.e., one equipped with the JAVAD receivers and the other with the Trimble receivers. Figure 7 shows the

Table 3 Statistical results of WL and NL residuals in the global network on DOY 152 of 2021

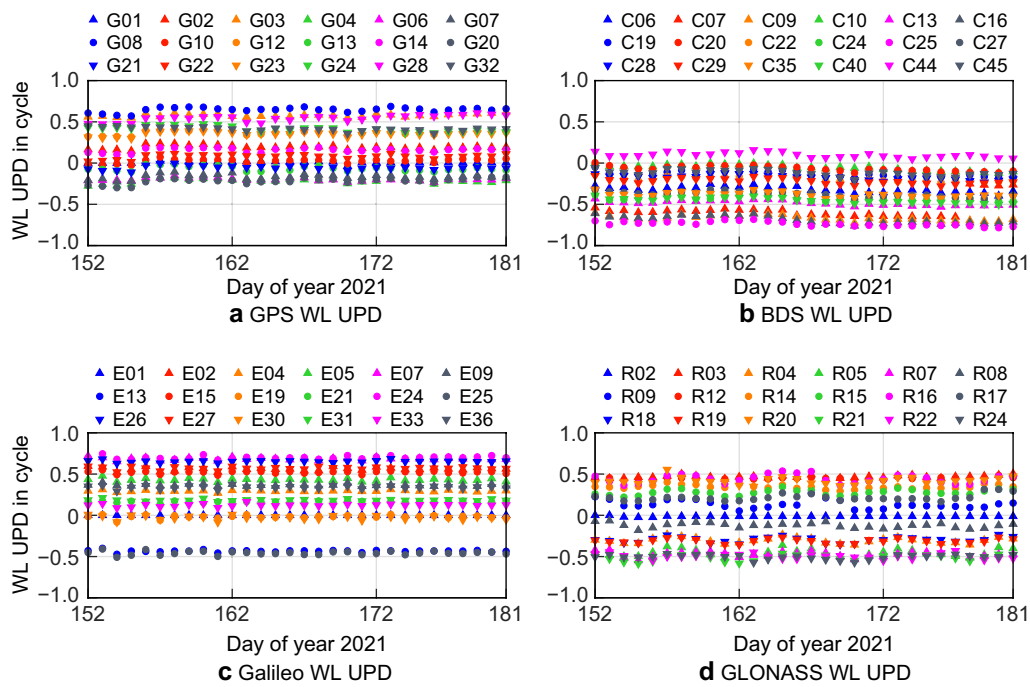| System	WL residuals in the global network				NL residuals in the global network			
	Mean in cycle	STD in cycle	Within ± 0.15 cycles (%)	Within ± 0.25 cycles (%)	Mean in cycle	STD in cycle	Within ± 0.15 cycles (%)	Within ± 0.25 cycles (%)
GPS	0.002	0.081	91.8	98.7	− 0.001	0.103	83.4	99.9
BDS	− 0.004	0.103	84.4	97.1	0.004	0.107	82.0	99.9
Galileo	0.004	0.062	96.1	99.4	− 0.004	0.102	84.5	99.9
GLONASS	− 0.006	0.138	69.6	92.7	− 0.001	0.104	83.9	99.8

Fig. 7 GPS (**a**), BDS (**b**), Galileo (**c**), and GLONASS (**d**) WL UPDs estimated in the regional network with JAVAD receivers from DOY 152 to 181 of 2021
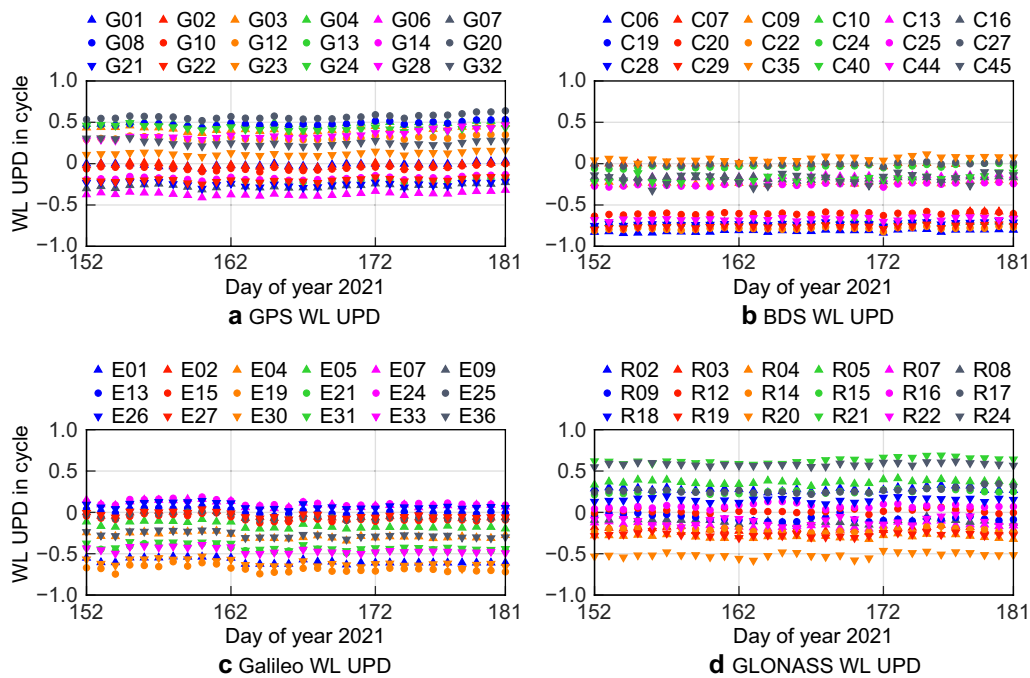

Fig. 8 GPS (**a**), BDS (**b**), Galileo (**c**), and GLONASS (**d**) WL UPDs estimated in the regional network with Trimble receivers from DOY 152 to 181 of 2021

systems have similar distributions of WL residuals. Table 5 shows that Galileo exhibits the best performance in terms of the distribution of the residuals with the STDs approximately

0.080 cycles. Specifically, 91.9% of the residuals are within ±0.15 cycles, and 99.2% within ±0.25 cycles.

Table 4 Usage rates of WL float ambiguities in the two regional networks on DOY 152 of 2021

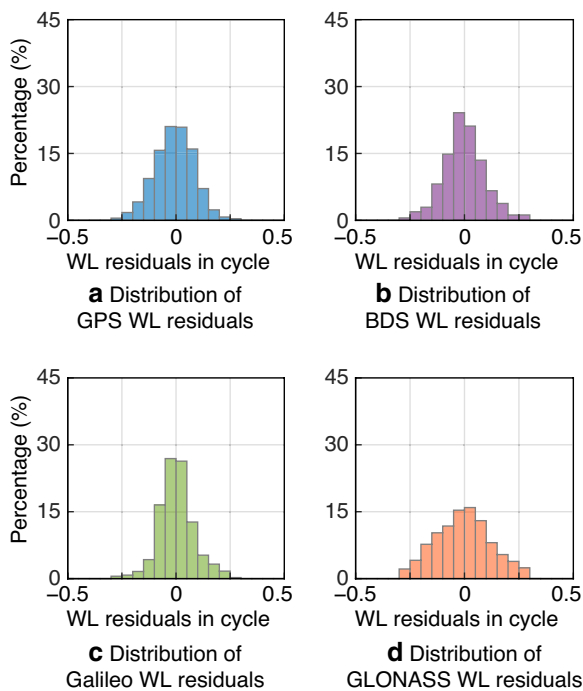| System	WL usage rates in the regional network with JAVAD receivers (%)			WL usage rates in the regional network with Trimble receivers (%)		
	Average	Maximum	Minimum	Average	Maximum	Minimum
GPS	100	100	100	99.6	100	96.7
BDS	96.0	100	65.4	92.3	100	83.3
Galileo	100	100	100	98.7	100	93.3
GLONASS	95.9	100	69.2	92.0	100	76.7

Fig. 9 Histogram of the GPS (**a**), BDS (**b**), Galileo (**c**), and GLONASS (**d**) WL residuals in the regional network with JAVAD receivers on DOY 152 of 2021
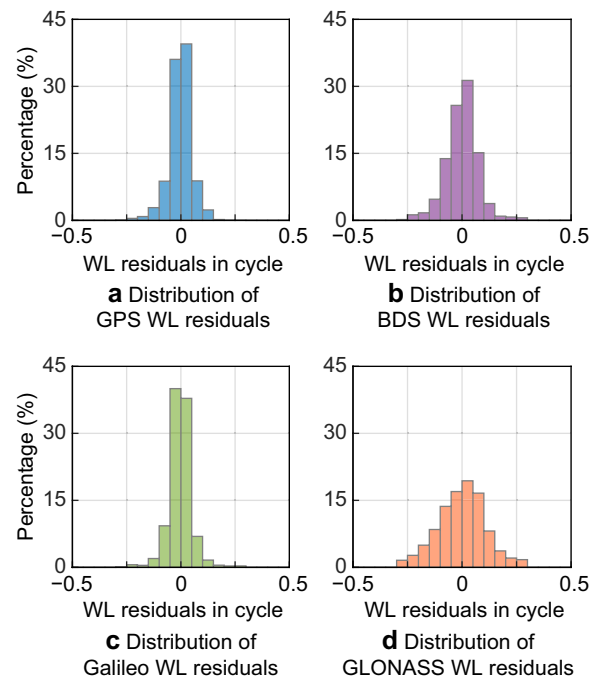

Fig. 10 Histogram of the GPS (**a**), BDS (**b**), Galileo (**c**), and GLONASS (**d**) WL residuals in the regional network with Trimble receivers on DOY 152 of 2021

Figure 10 shows the distribution of WL ambiguities residuals in the network with Trimble receivers. Comparing Figs. 9 and 10, we can find that the distribution of WL ambiguities residuals has some difference between the two regional networks. The STDs for four satellite systems in the network with Trimble receivers are smaller than those with JAVAD receivers. It indicates that the accuracy of UPDs is related to receiver types. Moreover, the receiver and satellite UPDs are estimated together by LS criterion. Considering the stability of the receiver hardware delays depends on receiver types, the receiver-dependent bias also can contaminate the satellite UPD estimates. Thus, applying homogeneous receivers is an effective method to improve UPD estimation accuracy.

Figure 11 shows the series of the daily NL UPDs generated in the network with JAVAD receivers on DOY 152 of 2021. The mean STDs for GPS, BDS, Galileo, and GLONASS are approximately 0.042, 0.034, 0.071, and 0.046 cycles, respectively. For another network, the NL UPDs estimated with Trimble receivers are shown in Fig. 12. The correspinding mean STDs are approximately 0.017, 0.030, 0.021, and 0.020 cycles. These results indicate that the NL UPDs have a significant difference between two networks with different receiver types. Also, we can find that the GPS, BDS, and GLONASS NL UPDs estimated in the networks with Trimble receivers are more stable than those with JAVAD receivers. It indicates that the hardware delays of these two receiver types are different, which will influence the satellites UPD estimation.

Table 5 Statistical results of WL residuals from the two regional networks on DOY 152 of 2021

System	WL residuals in the regional network with JAVAD receivers				WL residuals in the regional network with Trimble receivers			
	Mean in cycle	STD in cycle	within ± 0.15 cycles (%)	within ± 0.25 cycles (%)	Mean in cycle	STD in cycle	within ± 0.15 cycles (%)	within ± 0.25 cycles (%)
GPS	− 0.009	0.091	90.3	99.1	− 0.002	0.052	98.5	99.9
BDS	− 0.002	0.095	88.5	98.3	− 0.001	0.074	94.7	99.3
Galileo	0.002	0.080	91.9	99.2	− 0.003	0.053	97.8	99.5
GLONASS	− 0.006	0.125	74.6	95.4	− 0.001	0.109	83.4	96.7

Ignoring the stability of UPD will affect the results of estimated parameters. Specifically, it is not sufficient to regard UPD as a time-varying parameter in single epoch estimation. When the characteristics of UPDs are inconsistent with the prior assumptions, the accuracy will be reduced. Hence, it is important to select a suitable estimation method that can account for their dynamic characteristics when UPD parameters exhibit time-varying characteristics. This situation is more obvious in the regional network. Therefore, the solution mode or strategies need to be modified according to actual situations.

The usage rates of NL float ambiguities in the two regional networks are given in Table 6. We can find that the average usage rates in the network with JAVAD receivers for GPS, BDS, Galileo, and GLONASS are 93.7%, 91.5%, 96.5%, and 75.1%, respectively, while in the network with Trimble receivers are 91.0%, 87.3%, 94.8%, and 83.1%. Except for GLONASS, the usage rates of NL float ambiguities in the network with JAVAD receivers are higher than those in the network with Trimble receivers.

The statistical results of NL ambiguities residuals for two networks are given in Table 7. The residual STDs of the network with JAVAD receivers are approximately 0.050 cycles, while almost 0.100 cycles in another network. We can find that four satellite systems have the similar distribution of NL residuals, and the NL residuals for JAVAD receivers are more concentrated towards zero than Trimble. It is reasonable because the usage rates of NL ambiguities for Trimble are lower than JAVAD. Therefore, to ensure the optimal solution mode and strategies, it is crucial to have an adequate amount of data for UPD estimation.

Analysis of UPD estimators considering the impacts of network scales

The UPDs generated in different network scales also have different properties. By comparing the Figs. 3 and 7, and 8, we can find that the GPS, BDS, and Galileo WL UPDs which estimated in global and regional networks have the similar accuracy. It demonstrates that the WL UPDs are not sensitive to the unmodeled errors due to its long wavelength. For the NL UPDs, there are distinct differences between global and regional networks. By comparing the Figs. 4 and 11, we can find that the STDs of NL UPDs estimated in the global network for GPS, BDS, Galileo, and GLONASS are approximately 0.075, 0.096, 0.080, and 0.099 cycles, respectively, while the NL UPDs estimated in the regional network with JAVAD receivers are 0.042, 0.034, 0.071, and 0.046 cycles. The temporal stability for Galileo is not improved obviously because some satellites do not have many redundant observations. For the regional network with Trimble receivers, the NL UPDs are more stable than those in the global network. The STDs of GPS, BDS, Galileo, and GLONASS are approximately 0.017, 0.030, 0.021, and 0.020 cycles, respectively. The temporal stability is improved by 76.9%, 68.9%, 73.6% and 71.8%.

In addition, comparing Tables 3 and 7, we can find that the NL UPD residuals of four satellite systems are approximately 0.100 cycles in the global network, while the corresponding results in the regional network with JAVAD receivers are less than 0.060 cycles, and the accuracy is improved by more than 40.0%. For another regional network with Trimble receivers, the NL UPD residuals are at the same level as the global network, even though the usage rates of ambiguities are lower. It demonstrates that the temporal stability and residual distribution of the NL UPDs estimated in a regional network are generally better than those in the global network. These results can be attributed to different implication levels of the unmodeled errors at different network scales. Specifically, the unmodeled errors such as residual orbit errors and atmospheric delays in a small network are similar for each station. Hence, these unmodeled errors can be absorbed into the NL UPD estimates, providing higher accuracy for UPD estimators.

Furthermore, the NL UPDs estimated in the global network are available any time, while the corresponding results in the regional networks are discontinuous and dependent on the visible satellites. The main reason
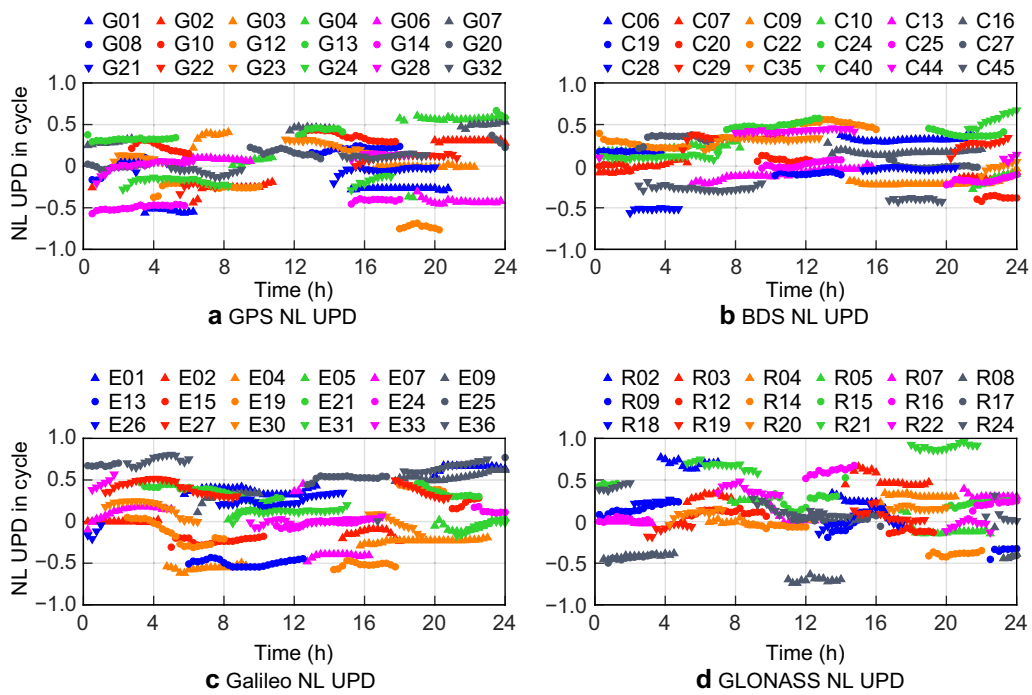
Fig. 11 GPS (**a**), BDS (**b**), Galileo (**c**), and GLONASS (**d**) NL UPDs estimated in the regional network with JAVAD receivers on DOY 152 of 2021
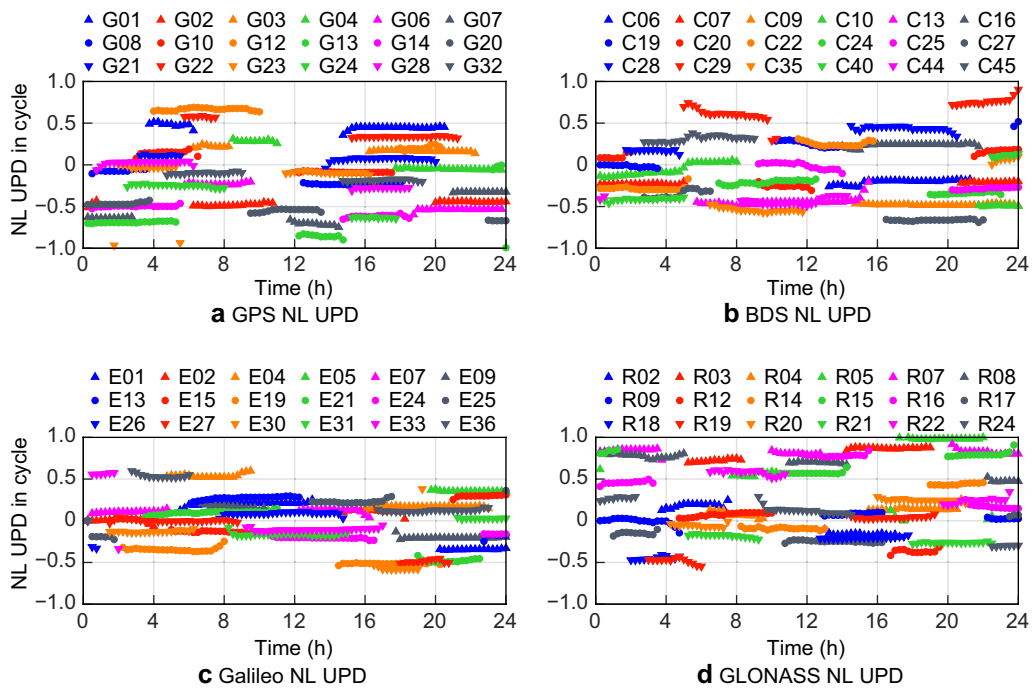

Fig. 12 GPS (**a**), BDS (**b**), Galileo (**c**), and GLONASS (**d**) NL UPDs estimated in the regional network with Trimble receivers on DOY 152 of 2021

Table 6 Usage rate of NL float ambiguities in the two regional networks on DOY 152 of 2021

System	NL usage rates in the regional network with JAVAD receivers (%)			NL usage rates in the regional network with Trimble receivers (%)		
	Average	Maximum	Minimum	Average	Maximum	Minimum
GPS	93.7	95.9	90.9	91.0	97.7	81.2
BDS	91.5	96.1	69.6	87.3	97.8	73.6
Galileo	96.5	98.7	93.7	94.8	97.6	90.0
GLONASS	75.1	83.0	65.8	83.1	90.9	67.3

Table 7 Statistical results of NL residuals in the two regional networks on DOY 152 of 2021

System	NL residuals in the regional network with JAVAD receivers				NL residuals in the regional network with Trimble receivers			
	Mean in cycle	STD in cycle	within $\pm$ 0.15 cycles (%)	Within $\pm$ 0.25 cycles (%)	Mean in cycle	STD in cycle	Within $\pm$ 0.15 cycles (%)	Within $\pm$ 0.25 cycles (%)
GPS	0.001	0.054	97.7	99.9	0.001	0.089	89.7	99.9
BDS	0.002	0.061	95.8	99.9	0.005	0.099	85.4	99.7
Galileo	$-$ 0.004	0.054	97.6	100	$-$ 0.002	0.085	91.4	100
GLONASS	$-$ 0.002	0.056	96.6	99.9	0.001	0.098	86.3	99.9

is that the global network has a longer visible arc than regional network. Thus, the UPDs estimated in the global network can provide continuous service for users, while the UPDs estimated in the regional network are theoretically more suitable for local users due to the less unmodeled errors.

Conclusions and outlook

We comprehensively interpret the properties of the UPDs by considering the impacts of different satellite systems, receiver types, and network scales. We collected the observations of MGEX and EUREF from June 1st to 30th in 2021 and divided the EUREF into two networks with different receiver types. To analyze the impacts of different satellite systems in UPD estimation, we generated the WL and NL UPDs of four satellite systems, i.e., GPS, BDS, Galileo, and GLONASS.

The main concluding remarks are as follows. First, the different satellite systems exhibit different characteristics in UPD estimation. The main attributions include the precise product, signal type, and signal quality. Therefore, the estimation method, update frequency, and solution mode of UPD need to be treated differently for different satellite systems. Second, different receiver types also impact the UPD estimation. Because the receiver and satellite UPDs are estimated together using the LS criterion, the estimated satellite UPDs can affected by receiver-dependent biases, such as residuals of antenna phase center offset and receiver noise. In addition, due to the different receiver-specific

hardware delays, it is inappropriate for traditional methods to ignore receiver-dependent bias and just treat UPDs as time-varying parameters. As a result, we suggest that users select homogeneous receiver type when estimating UPDs if possible. Third, different network scales exhibit the different implication of unmodeled errors. In general, the unmodeled errors tend to be more similar for the stations in a small network and can be absorbed into the procedure of UPD estimation, particularly for the NL UPDs. Theoretically, the UPD estimated in the regional network is more beneficial for regional users. Hence, different users can choose the appropriate network scale for the generation of UPDs according to their own needs.

Abbreviations

AC	Analysis Center
AR	Ambiguity Resolution
DOY	Day of Year
BDS	BeiDou Navigation Satellite System
BDS-2	BeiDou-2 Navigation Satellite System
BDS-3	BeiDou-3 Navigation Satellite System
CODE	Center for Orbit Determination in Europe
DCB	Differential Code Bias
EUREF	Europe Reference Frame
Galileo	Galileo navigation satellite system
GFZ	Deutsches GeoForschungsZentrum Potsdam
GLONASS	GLObal NAvigation Satellite System
GMF	Global Mapping Function
GNSS	Global Navigation Satellite System
GPS	Global Positioning System
IERS	International Earth Rotation Service
IF	Ionosphere-Free
IFB	Inter-Frequency Bias

IGS	International GNSS Service
IGSO	Inclined Geosynchronous Orbit
ISB	Inter-System Bias
LS	Least Squares
MEO	Medium Earth Orbit
MGEX	Multi-GNSS EXperiment
MW	Melbourne-Wübeena
NL	Narrow-Lane
PCO	Phase Center Offset
PCV	Phase Center Variation
PPP	Precise Point Positioning
STD	STandard Deviation
UPD	Uncalibrated Phase Delay
WL	Wide-Lane
ZWD	Zenith Wet Delay

Availability of data and materials
The GNSS raw data of MGEX and EUREF can be accessed from ftp://igs.gnsswhu.cn/pub/gps/data/daily/ and ftp://igs.bkg.bund.de/EUREF/obs/, respectively. The GFZ final products are available at ftp://ftp.gfz-potsdam.de/GNSS/products/mgex/. The DCB products are from ftp://ftp.aiub.unibe.ch/CODE/. The IGS antenna corrections can be accessed from https://files.igs.org/pub/station/general/.

Declarations

Competing interests
The authors declare that they have no conflict of interest.

References

Blewitt, G. (1998). GPS data processing methodology: From theory to applications. In P. Teunissen, & A. Kleusberg (Eds.), *GPS for geodesy*. Berlin: Springer.

Blewitt, G. (2008). Fixed point theorems of GPS carrier phase ambiguity resolution and their application to massive network processing: Ambizap. *Journal Geophysical Research: Solid Earth, 113*(B12), B12410.

Collins, P., Lahaye, F., Héroux, P., & Bisnath, S. (2008). Precise point positioning with ambiguity resolution using the decoupled clock model. In *Proceedings of ION GNSS 2008, Savannah* (pp. 1315–1322).

Cui, B., Li, P., Wang, J., Ge, M., & Schuh, H. (2021). Calibrating receiver-type-dependent wide-lane uncalibrated phase delay biases for PPP integer ambiguity resolution. *Journal of Geodesy, 95*(7), 82.

Gabor, M., & Nerem, R. (1999). GPS carrier phase ambiguity resolution using satellite-satellite single differences. In *Proceedings of ION GPS 1999, Nashville city* (pp. 1569–1578).

Ge, M., Gendt, G., Rothacher, M., Shi, C., & Liu, J. (2008). Resolution of GPS carrier-phase ambiguities in Precise Point Positioning (PPP) with daily observations. *Journal of Geodesy, 82*(7), 389–399.

Geng, J., Chen, X., Pan, Y., Mao, S., Li, C., Zhou, J., & Zhang, K. (2019a). PRIDE PPP-AR: An open-source software for GPS PPP ambiguity resolution. *GPS Solutions, 23*(4), 91.

Geng, J., Chen, X., Pan, Y., & Zhao, Q. (2019b). A modified phase clock/bias model to improve PPP ambiguity resolution at Wuhan University. *Journal of Geodesy, 93*(10), 2053–2067.

Geng, J., Shi, C., Ge, M., Dodson, A., Lou, Y., Zhao, Q., & Liu, J. (2012). Improving the estimation of fractional-cycle biases for ambiguity resolution in precise point positioning. *Journal of Geodesy, 86*(8), 579–589.

Inazu, D., Waseda, T., Hibiya, T., & Ohta, Y. (2016). Assessment of GNSS-based height data of multiple ships for measuring and forecasting great tsunamis. *Geoscience Letters, 3*, 25.

Jin, S., & Su, K. (2019). Co-seismic displacement and waveforms of the 2018 Alaska earthquake from high-rate GPS PPP velocity estimation. *Journal of Geodesy, 93*(9), 1559–1569.

Ju, B., Jiang, W., Tao, J., Hu, J., Xi, R., Ma, J., & Liu, J. (2022). Performance evaluation of GNSS kinematic PPP and PPP-IAR in structural health monitoring of bridge: Case studies. *Measurement, 203*, 112011.

Kouba, J., & Héroux, P. (2001). Precise point positioning using IGS orbit and clock products. *GPS Solutions, 5*(2), 12–28.

Khodabandeh, A., & Teunissen, P. (2015). An analytical study of PPP-RTK corrections: Precision, correlation and user-impact. *Journal of Geodesy, 89*(11), 1109–1132.

Laurichesse, D., Mercier, F., Berthias, J., Broca, P., & Cerri, L. (2009). Integer ambiguity resolution on undifferenced GPS phase measurements and its application to PPP and satellite precise orbit determination. *Navigation, 56*(2), 135–149.

Leick, A., Rapoport, L., & Tatarnikov, D. (2015). *GPS satellite surveying*. London: Wiley.

Li, B., Zhang, Z., Shen, Y., & Yang, L. (2018). A procedure for the significance testing of unmodeled errors in GNSS observations. *Journal of Geodesy, 92*(10), 1171–1186.

Li, P., Zhang, X., & Guo, F. (2017). Ambiguity resolved precise point positioning with GPS and BeiDou. *Journal of Geodesy, 91*(1), 25–40.

Li, X., Huang, J., Li, X., Lyu, H., Wang, B., Xiong, Y., & Xie, W. (2021). Multi-constellation GNSS PPP instantaneous ambiguity resolution with precise atmospheric corrections augmentation. *GPS Solutions, 25*(3), 107.

Liu, Y., Ye, S., Song, W., Lou, Y., & Chen, D. (2017). Integrating GPS and BDS to shorten the initialization time for ambiguity-fixed PPP. *GPS Solutions, 21*(2), 333–343.

Liu, S., & Yuan, Y. (2022). Generating GPS decoupled clock products for precise point positioning with ambiguity resolution. *Journal of Geodesy, 96*, 6.

Melbourne, W. (1985). The case for ranging in GPS-based geodetic systems. In *Proceedings of the first international symposium on precise positioning with the Global Positioning System. Rockville City* (pp. 373–386).

Schaer, S., Villiger, A., Arnold, D., Dach, R., Prange, L., & Jäggi, A. (2021). The CODE ambiguity-fixed clock and phase bias analysis products: Generation, properties, and performance. *Journal of Geodesy, 95*(7), 81.

Schmid, R., Rothacher, M., Thaller, D., & Steigenberger, P. (2005). Absolute phase center corrections of satellite and receiver antennas. *GPS Solutions, 9*(4), 283–293.

Shinghal, G., & Bisnath, S. (2021). Conditioning and PPP processing of smartphone GNSS measurements in realistic environments. *Satellite Navigation, 2*, 10.

Teunissen, P., & Montenbruck, O. (2017). *Springer handbook of global navigation satellite systems*. Cham: Springer.

Teunissen, P., Odijk, D., & Zhang, B. (2010). PPP-RTK: Results of CORS network-based PPP with integer ambiguity resolution. *Journal of Aeronautics, Astronautics and Aviation, Series A, 42*(4), 223–230.

Wanninger, L., & Beer, S. (2015). BeiDou satellite-induced code pseudorange variations: Diagnosis and therapy. *GPS Solutions, 19*(4), 639–648.

Wu, J., Wu, S., Hajj, G., Bertiger, W., & Lichten, S. (1993). Effects of antenna orientation on GPS carrier phase. *Manuscripta Geodaetica, 18*(2), 91–98.

Wübbena, G. (1985). Software developments for geodetic positioning with GPS using TI 4100 code and carrier measurements. In *Proceedings of the first international symposium on precise positioning with the Global Positioning System, Maryland City* (pp. 403–412).

Zeng *et al. Satellite Navigation*   (2023) 4:19

Page 15 of 15

Yang, Y., Mao, Y., & Sun, B. (2020). Basic performance and future developments of BeiDou global navigation satellite system. *Satellite Navigation, 1*, 1.

Zhang, B., Teunissen, P., & Odijk, D. (2011). A novel un-differenced PPP-RTK concept. *Journal of Navigation*, *64*(S1), S180–S191.

Zhang, X., & Li, P. (2013). Assessment of correct fixing rate for precise point positioning ambiguity resolution on a global scale. *Journal of Geodesy, 87*(6), 579–589.

Zhang, Z., Yuan, H., Li, B., He, X., & Gao, S. (2021). Feasibility of easy-to-implement methods to analyze systematic errors of multipath, differential code bias, and inter-system bias for low-cost receivers. *GPS Solutions, 25*(3), 116.

Zheng, K., Zhang, X., Sang, J., Zhao, Y., Wen, G., & Guo, F. (2021). Common-mode error and multipath mitigation for subdaily crustal deformation monitoring with high-rate GPS observations. *GPS Solutions, 25*(2), 67.

Zumberge, J., Heflin, M., Jefferson, D., Watkins, M., & Webb, F. (1997). Precise point positioning for the efficient and robust analysis of GPS data from large networks. *Journal Geophysical Research: Solid Earth, 102*(B3), 5005–5017.

Publisher's Note